Published in final edited form as:
Sci Signal. ; 1(36): ra3. doi:10.1126/scisignal.1161577.

Phosphoinositide 3-Kinase p110β activity: Key Role in Metabolism and Mammary Gland Cancer but not Development

Elisa Ciraolo[1], **Manuela Iezzi**[4], **Romina Marone**[3], **Stefano Marengo**[1], **Claudia Curcio**[2], **Carlotta Costa**[1], **Ornella Azzolino**[1], **Cristiano Gonella**[1], **Cristina Rubinetto**[1], **Haiyan Wu**[5], **Walter Dastrù**[6], **Erica L. Martin**[7], **Lorenzo Silengo**[1], **Fiorella Altruda**[1], **Emilia Turco**[1], **Letizia Lanzetti**[8], **Piero Musiani**[4], **Thomas Rückle**[9], **Christian Rommel**[9], **Jonathan M. Backer**[5], **Guido Forni**[2], **Matthias P. Wymann**[3], and **Emilio Hirsch**[1,*]

[1] *Molecular Biotechnology Center. Department of Genetics, Biology and Biochemistry. University of Torino. Via Nizza 52. 10126 Torino. Italy* [2] *Molecular Biotechnology Center. Department of Clinical and Biological Sciences, University of Torino. 10126 Torino. Italy* [3] *Inst. Biochemistry and Genetics, Dept. Biomedicine University of Basel, Mattenstrasse 28. CH-4058 Basel. Switzerland* [4] *Aging Research Centre. G. d'Annunzio University Foundation. Chieti. Italy* [5] *Department of Molecular Pharmacology. Albert Einstein College of Medicine. Bronx, NY. USA* [6] *Department of Chemistry IFM, via P. Giuria, 7. Molecular Imaging Center, via Nizza 52. University of Torino. Torino. Italy* [7] *Department of Anesthesia and Critical Care. University of Torino. Corso Dogliotti 14. 10126 Torino. Italy* [8] *Dipartimento di Scienze Oncologiche. University of Torino. Istituto per la Ricerca e la Cura del Cancro, Str. Provinciale 142, 10060 Candiolo, Torino, Italy* [9] *Merck Serono S.A. Geneva Research Center, Geneva. Switzerland*

Abstract

The phosphoinositide 3-kinase (PI3K) pathway crucially controls metabolism and cell growth. Although different PI3K catalytic subunits are known to play distinct roles, the specific in vivo function of p110β (the product of the *PIK3CB* gene) is not clear. Here, we show that mouse mutants expressing a catalytically inactive *PIK3CB*^{K805R} mutant survived to adulthood but showed growth retardation and developed mild insulin resistance with age. Pharmacological and genetic analyses of p110β function revealed that p110β catalytic activity is required for PI3K signaling downstream of heterotrimeric guanine nucleotide-binding (G protein)-coupled receptors as well as to sustain long term insulin signaling. In addition, *PIK3CB*^{K805R} mice were protected in a model of *ERBB2*-driven tumor development. These findings indicate an unexpected role for p110β catalytic activity in diabetes and cancer, opening potential new avenues for therapeutic intervention.

Introduction

Phosphoinositide 3-kinases (PI3Ks) and their lipid product phosphatidylinositol-3,4,5-trisphosphate [PtdIns(3,4,5)P_3] are involved in signaling events influencing a large number of cellular processes (1–3). Class I_A PI3Ks are mainly activated by receptor tyrosine kinases (RTKs) and form heterodimers composed of a catalytic subunit (p110α, β, or δ, which are encoded by the *PIK3CA*, *PIK3CB,* and *PIK3CD* genes, respectively) and a SH2 domain-containing adaptor protein (p85α, p50α, p55α, p85β or p55γ) (3). Class I_A PI3Ks are activated

*To whom correspondence should be addressed; E-mail: E-mail: emilio.hirsch@unito.it.

by either p85 recruitment to phosphorylated RTKs and adaptors like insulin receptor substrate 1 and 2 (IRS-1/2) or by binding to Ras (2). Whereas p110α is known to play a major role in insulin signaling (4,5), and p110δ in lymphocyte activation (6), the role of p110β has remained elusive. Pharmacological studies have suggested a role for p110β in platelet aggregation (7); however, the early embryonic lethal phenotype caused by its genetic ablation (8) has prevented accurate characterization of its in vivo function.

Aberrant regulation of the PI3K signaling pathway is frequently associated with cancer (9). Mutations in the class IA p110 gene *PIK3CA* can be detected in a number of human tumors (10,11). Although mutations in p110β corresponding to oncogenic p110α mutations fail to elicit the same oncogenic behavior (12), overexpression of wild-type p110β induces transformation in cultured cells (13) and various human cancers show increased abundance of p110β (14). Nonetheless, whether targeting p110β could be effective in cancer therapy is unknown.

Here, we show that mice expressing a catalytically inactive form of p110β survive to adulthood and develop a mild insulin resistance with age. Mutant mice were protected in an in vivo model of *ERBB2*-driven mammary gland cancer development, identifying p110β as a promising drug target with tolerable side effects.

Results

Generation of mice expressing a kinase-dead p110β mutant

A mouse strain was engineered to carry a mutation in the *PIK3CB* gene (Suppl. Fig. 1) in which Lys805 of the p110β ATP-binding site was replaced with Arg (*PIK3CB*^{K805R} allele), leading to the production of a catalytically inactive form of p110β (p110β^{K805R}). Unexpectedly, homozygous *PIK3CB*$^{K805R/K805R}$ mice were viable and reached adulthood. However, 50% fewer *PIK3CB*$^{K805R/K805R}$ mice were born from heterozygous crosses than expected (50 mutant homozygotes out of 372 mice analyzed; $P<0.0001$ by χ^2), indicating embryonic lethality with incomplete penetrance. This phenotype could not be associated to expression of aberrant p110β variants still retaining partial catalytic activity (Suppl. Fig. 2a–e).

Unexpected non-catalytic function of p110β

At embryonic day 13.5, two distinct groups of *PIK3CB*$^{K805R/K805R}$ littermate embryos were found: approximately 70% appeared normal, whereas approximately 30% were abnormally small and moribund. The existence of these two distinct groups appeared to be related to genetic background because increased contribution of the C57/BL6J background resulted in a marked decrease in the percentage of normal homozygous embryos. In murine embryonic fibroblasts (MEFs) derived from these two mutant populations, the protein and mRNA abundance of p110β^{K805R} was different (Fig. 1a, b and Suppl. Fig. 2g); it reached 60 to 80% of control amounts in normal embryos (*PIK3CB*$^{K805R/K805R\ High}$) but only 5 to 20% of wild-type p110β amounts in abnormal embryos (*PIK3CB*$^{K805R/K805R\ Low}$). In MEFs from *PIK3CB*$^{K805R/K805R\ High}$, enzymatic activity of p110β^{K805R} did not increase above background (Fig. 1c and d) however p110α and p85 expression were not altered from that in wild-type MEFs (Fig. 1a and b). Similarly, both total class IA PI3K activity, precipitated with beads linked to a phosphopeptide that mimicked an activated growth factor receptor (Fig. 1d, Suppl. Fig 2f), and p110α activity, immunoprecipitated with antibodies directed against p110α, (Suppl. Fig 2f) were normal, showing that the in vitro activity of other class IA PI3Ks was unaltered. Further, decreased p110β abundance did not cause any substantial increase in free p85 (Suppl. Fig. 3).

Lack of p110β leads to early embryonic lethality associated with defective cell proliferation (8) and, in agreement, impaired cell proliferation was found in *PIK3CB*$^{K805R/K805R\ Low}$ MEFs. In contrast, *PIK3CB*$^{K805R/K805R\ High}$ cells unexpectedly proliferated at a rate similar to that of wild-type MEFs (Fig. 1e). Consistent with this, cell proliferation of wild-type MEFs did not change after treatment with the p110β-selective inhibitors TGX-221 (7) (Fig. 1e) or TGX-155 (15) (Suppl. Fig. 4), suggesting a non-catalytic function of p110β. p110β is known to associate with Rab5, a monomeric small guanosine triphosphatase (GTPase) involved in fusion of clathrin-coated vesicles and in growth factor receptor endocytosis (16,17). We thus investigated the possible role of p110β in these processes. We found that, although the amount of plasma membrane epidermal growth factor receptor (EGFR) was similar in mutant and control cells, internalization of epidermal growth factor (EGF)-activated EGFR in *PIK3CB*$^{K805R/K805R\ Low}$ cells was impaired compared to both wild-type and *PIK3CB*$^{K805R/K805R\ High}$ cells (Fig. 2a).

Overexpression of a dominant-active Rab5 mutant (Rab5Q79L) did not rescue EGFR internalization in the *PIK3CB*$^{K805R/K805R\ Low}$ MEFs (Suppl. Fig. 5), suggesting a role of p110β at early steps of endocytosis. Consistently, *PIK3CB*$^{K805R/K805R\ Low}$ MEFs showed a decrease in the numbers of clathrin-positive vesicles beneath the plasma membrane compared to control cells. In contrast, clathrin staining in the perinuclear region was not affected (Fig. 2b). Moreover, recruitment of the Rab5 effector early endosomal antigen 1 (EEA1) to early endosomes was reduced in *PIK3CB*$^{K805R/K805R\ Low}$ MEFs (Fig. 2b), likely as a consequence of alterations in the endocytic route.

Requirement for p110β catalytic function downstream of both receptor tyrosine kinases and G protein-coupled receptors

Comparison of wild-type and *PIK3CB*$^{K805R/K805R\ High}$ MEFs revealed that the catalytic function of p110β was not required for Akt activation 5 minutes after stimulation with insulin, insulin-like growth factor 1 (IGF-1), EGF, or platelet-derived growth factor (PDGF) (Fig. 3a and Suppl. Fig 6). Nonetheless, p110β catalytic activity in MEFs was required for lysophosphatidic acid (LPA)- and sphingosine-1-phosphate (S1P)-dependent phosphorylation of Akt (Fig. 3b and 3c), providing genetic evidence for the involvement of p110β in heterotrimeric guanine nucleotide-binding protein (G protein)-coupled receptor (GPCR) signaling, as previously suggested (5,18,19).

Despite the normal growth of *PIK3CB*$^{K805R/K805R\ High}$ MEFs in culture, *PIK3CB*$^{K805R/K805R}$ mice showed growth retardation, suggesting p110β involvement in growth control in vivo. *PIK3CB*$^{K805R/K805R}$ mice were born smaller than controls and showed an average 20% growth retardation that was compensated only after 24 weeks of age, at which time they did not show a significant reduction in muscle weight or alteration in fat mass (Fig. 3d and e, and Suppl. Fig. 7a and b). The abundance of p110β^{K805R} in various tissues, including liver, fat, and skeletal muscle, appeared lower than in controls but was never as low as in MEFs derived from abnormal embryos (Suppl. Fig. 7c). Mutant livers also displayed normal amounts of insulin receptor-β (IRβ) and IRS-1 (Suppl. Fig. 7d). In *PIK3CB*$^{K805R/K805R}$ liver extracts, p110β enzymatic activity was undetectable; however, PI3K activity precipitated by either anti-p110α antibodies or pan-p85 unselective antibodies or by phosphopeptide-linked beads (Suppl. Fig. 2f) was unaltered, suggesting normal in vitro activity of other class I_A PI3K. *PIK3CB*$^{K805R/K805R}$ mice developed increased blood glucose and signs of mild insulin resistance that was detectable from 6 months of age (Fig. 4a–f). This phenotype was accompanied by pancreatic islet hyperplasia and increased insulin secretion (Fig. 4g). Furthermore, mutant mice showed reduced hepatic glycogen deposits and defective insulin-mediated inhibition of gluconeogenesis (Fig. 4h–j), indicating that the mutation impacts insulin-mediated control of liver metabolism. Similarly, mutant mice showed decreased

expression of sterol regulatory element-binding protein factor 1C (SREBF-1c), a transcription factor that regulates the lipogenic program, as well as reduced serum triglycerides and cholesterol, demonstrating abnormal lipid metabolism in the liver and consequent dyslipidemia (Table I).

Because these findings appear inconsistent with a major role of p110α in insulin signaling (4, 5), we sought to define the molecular mechanism involved, by analyzing the signaling complex at the activated insulin receptor. In agreement with p110α being crucial for acute insulin receptor signaling, at early time points after insulin stimulation 8 week-old *PIK3CB*$^{K805R/K805R}$ livers showed normal recruitment of p85 and p110α to IRS-1 (Fig 5a) as well as unaltered p110α activity (Suppl. Fig. 7e) and Akt phosphorylation (Fig 5b). However, in livers of wild-type mice treated with TGX-155 or of *PIK3CB*$^{K805R/K805R}$ mice, insulin-evoked Akt activation declined significantly faster than in untreated wild-type controls (Fig. 5b). Similar results were observed in insulin-stimulated HepG2 hepatoma cells treated with TGX-221 (Suppl. Fig. 8).

Requirement for p110β in ERBB2-mediated mammary carcinogenesis

The observation that p110β catalytic function was required for insulin signaling suggested that this isoform could also be involved downstream of other growth factor receptors or their oncogenic forms. Because p110β can be activated downstream of EGFR (17,20) and is homogeneously expressed in the epithelium of mammary ducts (Fig. 6a), we studied the *PIK3CB*^{K805R} mutation in a model of breast cancer triggered by activated *ERBB2* (also known as HER-2 or neu) (21,22), an oncogene known to signal through an unidentified PI3K isoform (s) (23). *PIK3CB*$^{K805R/K805R}$ mice were intercrossed with BalbC transgenic mice expressing activated *ERBB2* (neuT) in the mammary gland. A cohort of 7 *PIK3CB*$^{K805R/K805R}$/neuT and 10 *PIK3CB*$^{WT/WT}$/neuT female mice was followed for 350 days. In agreement with whole mount preparations showing a strong reduction of the side buds at 10 weeks of age (Fig. 6c), development of the first tumor was substantially delayed in *PIK3CB*$^{K805R/K805R}$/neuT mice (Fig. 6b and Table II). Furthermore, at least up to 380 days of life, *PIK3CB*$^{K805R/K805R}$/neuT mice showed a reduced number of tumors (Suppl. Fig. 9a), which grew at a significantly lower rate than in *PIK3CB*$^{WT/WT}$/neuT controls (Table II and Suppl. Fig. 9b). Immunohistochemistry showed expression of activated *ERBB2* in both genotypes; however, the foci of transformation and the high numbers of proliferating Proliferating Cell Nuclear Antigen (PCNA)-positive cells, which completely filled duct lumina of *PIK3CB*$^{WT/WT}$/neuT mammary glands, were reduced in mutant samples, which showed empty and scarcely proliferating structures (Fig. 6d). To determine whether this protection was intrinsic to the function of p110β in mammary gland epithelium, cells from multiple primary tumors were bulk cultured in vitro. Immunostaining with antibodies directed against E-Cadherin confirmed that these cultures consisted of a homogeneous epithelial population (Suppl. Fig. 10). *PIK3CB*$^{K805R/K805R}$/neuT cells showed an average one third reduction in total p110β abundance but normal amounts of p110α and p85 (Fig. 7a). The development of tumors in compound-mutant mice correlated with mutations downstream of PI3K because a reduction in the amount of the PtdIns(3,4,5) P_3 phosphatase PTEN was detected in polyclonal *PIK3CB*$^{K805R/K805R}$/neuT tumors (Fig. 7a). Despite the decrease in PTEN abundance, *PIK3CB*$^{K805R/K805R}$/neuT cell populations grew significantly slower than controls (Fig. 7b). To test if this effect was due to either the lack of the kinase activity or the reduction in p110β^{K805R} expression, cells of both genotypes were cultured in the presence of p110βselective inhibitors, TGX-155 or TGX-221 (7,15,24) (Fig. 7b). This treatment did not show effects in *PIK3CB*$^{K805R/K805R}$/neuT cells but caused a significant reduction in proliferation in wild-type tumor cells, demonstrating that oncogenic ERBB2 drives tumor growth largely through p110β catalytic activity.

Discussion

Whereas PI3Ks-mediated signaling has been implicated in the control of cell proliferation, survival, and metabolism, the specific role of the p110β isoform has long remained elusive. We showed here that, unexpectedly, p110β possesses both kinase-dependent and independent functions. Indeed, our results indicate that p110β may have a scaffolding function, as already shown for the G protein-coupled p110γ (25). The kinase-independent function(s) of p110β are sufficient for embryonic development because low abundance of p110β protein led to embryonic lethality and the presence of p110β--even in a catalytically inactive form--was sufficient to allow embryonic development and viability to adulthood.

The existence of a multiprotein complex containing both p110β and Rab5 (16,17) suggests a potential function of p110β in clathrin-mediated endocytosis. Our results are consistent with p110β being mainly associated with clathrin-coated vesicles (16) and support the requirement for p110β kinase-independent activity early in the endocytic pathway. Indeed, our findings suggest that GTP-bound active-Rab5 recruits p110β to clathrin-coated pits or vesicles and that the scaffolding activity of p110β contributes to their assembly. In the absence of such scaffolding function clathrin-coated vesicles seem to be inefficiently formed. In turn, this appears to affect the Rab5-dependent endocytic pathway resulting in a decrease of EEA1-positive endosomes.

Despite the unexpected finding of its non-catalytic function, p110β kinase activity is clearly required downstream of both receptor tyrosine kinases and GPCRs. For example, GPCR signaling triggered by S1P and LPA required p110β to trigger Akt phosphorylation. This provides a simple mechanistic explanation for the apparently paradoxical ability of GPCRs to trigger PI3K signaling in cells not expressing p110γ, the prototypical GPCR-activated PI3K (26). Our findings are in agreement with recent reports (27,28) and with earlier pioneering studies indicating GPCR-mediated p110β activation (19) by direct association of p110β with the βγ dimer of heterotrimeric G proteins (18).

On the other hand, our data also indicate p110β catalytic function is required downstream of receptor tyrosine kinases and contributes to insulin receptor signaling. *Pik3cb*$^{K805R/K805R}$ mice show a mild increase in blood glucose and peripheral insulin resistance, which is accompanied by increased insulin secretion and pancreatic islet hyperplasia. This is consistent with a compensation typical of the hyperinsulinemia observed in patients with impaired glucose tolerance (29). In addition, decreased hepatic glycogen deposits and defective insulin-mediated inhibition of gluoconeogenesis indicate that the absence of p110β catalytic activity impacts insulin-mediated control of liver metabolism. Similarly, p110β is required for lipid metabolism and for the regulation of the lipogenic program as demonstrated by the decreased expression of SREBF-1c as well as reduced serum tryglicerides and cholesterol. These finding were unexpected because p110α is the main PI3K isoform known to be involved in insulin signaling (4,5). Nonetheless, consistent with our findings, reduced p110β expression correlates with the incidence of type 2 diabetes associated with low birthweight (30). Although p110α alpha plays a major role in the insulin signaling pathway, we demonstrate that p110β activity is essential to sustain a prolonged insulin stimulation. Mechanistically, this effect could perhaps be explained through the auto-inhibition of p110α, but not of p110β, following insulin stimulation (31). Although the limited extent of Akt phosphorylation impairment suggests a possible combination of kinase-dependent and independent functions of p110β in insulin signaling, our data show that the catalytic activity of p110β supports p110α function. Therefore, whereas the spike of PI3K signaling following insulin and growth factor stimulation depends on p110α (5), our results provide conclusive genetic evidence that p110β supports the PtdIns(3,4,5)P_3 production that sustains this response.

A similar mechanism could account for the reduced tumorigenicity associated with oncogenic *ERBB2* signaling. Previous reports have demonstrated that PI3K signaling is involved in ERBB2-mediated proliferation of mammary gland epithelium (32) but have also shown that mutations of the p110α-encoding PIK3CA gene are associated with *ERBB2* amplification, suggesting a link between p110α and ERBB2 signaling (33). However, as decreased proliferation is detected in *PIK3CB*$^{K805R/K805R}$/neuT compound mutant mammary glands, it is possible that, instead of p110α, p110β is the critical PI3K involved in *ERBB2*-positive cancer cell proliferation. PIK3CA mutation is mutually exclusive with the loss of the PtdIns(3,4,5) P_3 phosphatase PTEN (33) suggesting that p110α might play little role when PTEN is absent. In agreement, prostate cancer development triggered by PTEN loss is blocked by the lack of p110β and not p110α (27). Our data confirm and extend this idea, providing the first conclusive evidence that inhibition of the catalytic activity of p110β reduces proliferation of mammary gland cancer cells even in conditions of low PTEN abundance.

In conclusion, the data presented here indicate that the kinase-independent function(s) of p110β are sufficient for embryonic development but that p110β kinase activity is needed for normal insulin receptor signaling and for the growth of ERBB2-dependent mammary gland cancers (Fig. 8). These results suggest highly tissue-specific functions for p110β and indicate that p110β targeting could represent a promising option for treatment of selected tumors such as ERBB2-driven breast cancer.

Materials and methods

Mice

The targeting strategy used to generate the *PIK3CB*^{K805R} allele was similar to that previously used to generate the *PIK3CG*^{K833R} allele (25). Briefly, the point mutation leading to the substitution with an R of the K^{805} crucial for kinase activity was generated by site directed-mutagenesis of the *PIK3CB* cDNA and fused in frame with the *PIK3CB* 5th coding exon, followed by an internal ribosome entry site-enhanced Green Fluorescent Protein (IRES-eGFP) cassette and a pA signal. A Neo^{r}/HSV thymidine kinase selection cassette flanked by loxP sites was placed upstream of the mutant cDNA. To allow conditional expression of the kinase-dead p110β mutant, a duplicated *PIK3CB* 5th coding exon fused in frame with the *PIK3CB* wild-type cDNA and flanked by loxP sites was placed upstream of the selection cassette. The construct was electroporated in E14 embryonic stem (ES) cells and two independent recombinant clones were isolated. Heterozygous mice obtained from germ line chimeras were bred with Balancer Cre mice to delete the wild-type cDNA cassette and progeny were intercrossed to obtain *PIK3CB*$^{K805R/K805R}$ mice. Phenotypic analysis was carried out on two lines derived from independent clones. Results were obtained studying wild-type and mutant littermates derived from heterozygous crosses of mixed 50%129/Sv-C57Bl/6J-50%BalbC genetic background as well as in 9th generation C57Bl/6J (for diabetes studies) and 3rd generation BalbC (for cancer studies) backcrossed mice.

Reagents

The antibody directed against p110β was from S. Cruz Biotechnology (# sc-602). Antibodies directed against total Akt and P-Ser473 Akt were from a mouse monoclonal clone and from Cell Signaling Technology (#9271), respectively. Antibodies directed against p85 (#4257) and p110α (# 4254) were from Cell Signaling Technology. Antibodies directed against IRS-1 (#05–699) and insulin receptor α subunit (#07–724) were from Upstate.

Protein analysis

Tissues were removed, frozen in liquid nitrogen, and homogenized in lysis buffer (50mM Tris-HCl ph 8 and 150 mM NaCl) supplemented with 2 mg/ml aprotinin, 1 mM pepstatin, 1 ng/ml

leupeptin, 50 mM NaF, 2 mM Sodium O-vanadate, 1 mM sodium pyrophosphate, and 1% Triton X-100. The same buffer was used to solubilize protein extracts from cultured cells. Homogenates were clarified by centrifugation in a microcentrifuge at 4°C. Supernatant were analyzed for immunoblotting or immunoprecipitated for either 1h or overnight with the indicated antibodies. Immunocomplexes were bound to 30 μl of a suspension of 50% protein A- or protein G-Sepharose beads and washed with lysis buffer. Beads were resolved on SDS-PAGE and transferred on PVDF membranes. Blots were probed with the indicated antibodies and developed with enhanced chemiluminescence (ECL, Millipore).

Lipid kinase assay

p110α, p110β and pan-p85 were immunoprecipitated using specific antibodies. Alternatively, all class IA PI3K were pulled down with a phosphopeptide YpVPMLG corresponding to the consensus sequence next to Tyr 751 of the human PDGF receptor β. Proteins were then incubated with 10 mg of phosphatidyl inositol and radiolabeled ATP (10 mM cold ATP, 5 μCi P^{32} ATP). PtdIns(3)P products were resolved by thin-layer chromatography and visualized with autoradiography.

Endocytosis assays

Endocytosis assay was performed as described (34). Briefly, MEF cells were serum-starved for 2 hours in Dulbeccos's Modified Eagle Medium (DMEM) supplemented with 0.3% BSA. Cells were incubated with purified EGF (100 ng/ml Upstate Biotechnology Inc.) or fluorescently labelled EGF in DMEM supplemented with 0.3% BSA at 4 °C for 1 hour. The EGF-containing medium was then replaced with warm DMEM and cells were incubated at 37°C for a further 15 min. Cells were fixed with 4% paraformaldehyde in PBS for 10 min and permeabilized with 0.1% TritonX-100 in PBS for 10 min. Cells were extensively washed and stained with monoclonal anti-EGFR antibody (Oncogene Science, USA, catalog n. Ab-1), anti-EEA1 antibody (Santa Cruz, CA, USA, catalog n. SC6415), and anti-clathrin antibody (Affinity Bioreagents, CO, USA, catalog n. MA1-065) followed by Cy3-conjugated goat anti-mouse IgG (1:400 in PBS). Nuclei were stained with DAPI (Sigma). Time point 0 was obtained by fixing the cells after incubation with EGF at 4°C for 1 hour. Cells were stained without permeabilization as described above.

Cell culture and proliferation

For determination of relative growth, MEFs were seeded in triplicate at 2.5×10^5 cells per 6 cm tissue culture dish, with DMEM containing GlutaMAX and 4.5g/l glucose, (Invitrogen, USA) supplemented with 10% Fetal Bovine Serum (FBS). Cell numbers were evaluated using an automatic cell counter (Casy Technology, Germany). For measurement of tumor proliferation, cells were seeded in triplicate at 5×10^3 cells per 96 well dish and counted using an 3-(4,5-dimethyl thiazol-2-yl)-2,5-diphenyl tetrazolium bromide (MTT)-based colorimetric assay (Roche, Germany). Inhibitors of p110β were added to the culture 24 hours after plating. Data are the average of at least three independent experiments.

Metabolic studies

Measurements of body weight and length, glucose tolerance tests, and plasma insulin level determination were performed as previously described (35). Insulin tolerance tests were conducted on randomly fed (fed ad libitum) mice, by intraperitoneal injection of 1 U/kg of recombinant human insulin, followed by measurement of blood glucose at various time points. Plasma insulin was dosed using a RIA kit (#SRI-13K; LINCO Research, USA) following manufacturer's instructions. Measurement of other hematological parameters and quantitative polymerase chain reaction (PCR) were performed following standard protocols (36). Glycogen was measured as described (37).

Histological analysis

For pancreatic islet morphometric analysis, tissue was fixed in 10% neutral-buffered formalin, embedded in paraffin and cut into 5 μm thick sections. Sections were stained with haematoxylin and eosin following standard protocols. Islet area was measured with the Metamorph software in 8 sections 200 mM apart. Nuclei in each islet were counted and normalized to the measured area.

Histology, immunohistochemistry and mammary gland whole mount preparations were performed as previously described (38).

For mammary gland immunofluorescence analysis, mammary glands were fixed in PLP (4% paraformaldehyde, 0.2% periodate, 1.2% lysine in 0.1 M phosphate buffer), embedded in Optimum cutting temperature (OCT) freezing medium and cut into 5 μm thick sections. Fluorescently labeled 5g9 anti-p110β monoclonal antibody was obtained by coupling the purified Ig with Alexa Fluor® 488 (Pierce Biotechnology # 46403, IL, USA).

Statistical analysis

Statistical significance was calculated with Student's t, one or two-way ANOVA tests followed by Bonferroni's post hoc analysis, or Mantel-Haenszel Log-rank test where appropriate. Values are reported as the mean±standard error of the mean.

Supplementary Material

Refer to Web version on PubMed Central for supplementary material.

References and Notes

1. Wymann MP, Marone R. Phosphoinositide 3-kinase in disease: timing, location, and scaffolding. Curr Opin Cell Biol 2005;17:141–149. [PubMed: 15780590]
2. Engelman JA, Luo J, Cantley LC. The evolution of phosphatidylinositol 3-kinases as regulators of growth and metabolism. Nat Rev Genet 2006;7:606–619. [PubMed: 16847462]
3. Hirsch E, Costa C, Ciraolo E. Phosphoinositide 3-kinases as a common platform for multi-hormone signaling. J Endocrinol 2007;194:243–256. [PubMed: 17641274]
4. Foukas LC, Claret M, Pearce W, Okkenhaug K, Meek S, Peskett E, Sancho S, Smith AJ, Withers DJ, Vanhaesebroeck B. Critical role for the p110alpha phosphoinositide-3-OH kinase in growth and metabolic regulation. Nature 2006;441:366–370. [PubMed: 16625210]
5. Knight ZA, Gonzalez B, Feldman ME, Zunder ER, Goldenberg DD, Williams O, Loewith R, Stokoe D, Balla A, Toth B, Balla T, Weiss WA, Williams RL, Shokat KM. A pharmacological map of the PI3-K family defines a role for p110alpha in insulin signaling. Cell 2006;125:733–747. [PubMed: 16647110]
6. Okkenhaug K, Bilancio A, Farjot G, Priddle H, Sancho S, Peskett E, Pearce W, Meek SE, Salpekar A, Waterfield MD, Smith AJ, Vanhaesebroeck B. Impaired B and T cell antigen receptor signaling in p110delta PI 3-kinase mutant mice. Science 2002;297:1031–1034. [PubMed: 12130661]
7. Jackson SP, Schoenwaelder SM, Goncalves I, Nesbitt WS, Yap CL, Wright CE, Kenche V, Anderson KE, Dopheide SM, Yuan Y, Sturgeon SA, Prabaharan H, Thompson PE, Smith GD, Shepherd PR, Daniele N, Kulkarni S, Abbott B, Saylik D, Jones C, Lu L, Giuliano S, Hughan SC, Angus JA, Robertson AD, Salem HH. PI 3-kinase p110beta: a new target for antithrombotic therapy. Nat Med 2005;11:507–514. [PubMed: 15834429]
8. Bi L, Okabe I, Bernard DJ, Nussbaum RL. Early embryonic lethality in mice deficient in the p110beta catalytic subunit of PI 3-kinase. Mamm Genome 2002;13:169–172. [PubMed: 11919689]
9. Bader AG, Kang S, Zhao L, Vogt PK. Oncogenic PI3K deregulates transcription and translation. Nat Rev Cancer 2005;5:921–929. [PubMed: 16341083]

10. Bader AG, Kang S, Vogt PK. Cancer-specific mutations in PIK3CA are oncogenic in vivo. Proc Natl Acad Sci U S A 2006;103:1475–1479. [PubMed: 16432179]

11. Kang S, Bader AG, Vogt PK. Phosphatidylinositol 3-kinase mutations identified in human cancer are oncogenic. Proc Natl Acad Sci U S A 2005;102:802–807. [PubMed: 15647370]

12. Zhao JJ, Liu Z, Wang L, Shin E, Loda MF, Roberts TM. The oncogenic properties of mutant p110alpha and p110beta phosphatidylinositol 3-kinases in human mammary epithelial cells. Proc Natl Acad Sci U S A 2005;102:18443–18448. [PubMed: 16339315]

13. Kang S, Denley A, Vanhaesebroeck B, Vogt PK. Oncogenic transformation induced by the p110beta, -gamma, and -delta isoforms of class I phosphoinositide 3-kinase. Proc Natl Acad Sci U S A 2006;103:1289–1294. [PubMed: 16432180]

14. Benistant C, Chapuis H, Roche S. A specific function for phosphatidylinositol 3-kinase alpha (p85alpha-p110alpha) in cell survival and for phosphatidylinositol 3-kinase beta (p85alpha-p110beta) in de novo DNA synthesis of human colon carcinoma cells. Oncogene 2000;19:5083–5090. [PubMed: 11042696]

15. Robertson AD, Jackson S, Kenche V, Yaip C, Parbaharan H, Thompson P.

16. Christoforidis S, Miaczynska M, Ashman K, Wilm M, Zhao L, Yip SC, Waterfield MD, Backer JM, Zerial M. Phosphatidylinositol-3-OH kinases are Rab5 effectors. Nat Cell Biol 1999;1:249–252. [PubMed: 10559924]

17. Shin HW, Hayashi M, Christoforidis S, Lacas-Gervais S, Hoepfner S, Wenk MR, Modregger J, Uttenweiler-Joseph S, Wilm M, Nystuen A, Frankel WN, Solimena M, De Camilli P, Zerial M. An enzymatic cascade of Rab5 effectors regulates phosphoinositide turnover in the endocytic pathway. J Cell Biol 2005;170:607–618. [PubMed: 16103228]

18. Maier U, Babich A, Nurnberg B. Roles of non-catalytic subunits in gbetagamma-induced activation of class I phosphoinositide 3-kinase isoforms beta and gamma. J Biol Chem 1999;274:29311–29317. [PubMed: 10506190]

19. Murga C, Fukuhara S, Gutkind JS. A novel role for phosphatidylinositol 3-kinase beta in signaling from G protein-coupled receptors to Akt. J Biol Chem 2000;275:12069–12073. [PubMed: 10766839]

20. Lanzetti L, Palamidessi A, Areces L, Scita G, Di Fiore PP. Rab5 is a signalling GTPase involved in actin remodelling by receptor tyrosine kinases. Nature 2004;429:309–314. [PubMed: 15152255]

21. Guy CT, Webster MA, Schaller M, Parsons TJ, Cardiff RD, Muller WJ. Expression of the neu protooncogene in the mammary epithelium of transgenic mice induces metastatic disease. Proc Natl Acad Sci U S A 1992;89:10578–10582. [PubMed: 1359541]

22. Boggio K, Nicoletti G, Di Carlo E, Cavallo F, Landuzzi L, Melani C, Giovarelli M, Rossi I, Nanni P, De Giovanni C, Bouchard P, Wolf S, Modesti A, Musiani P, Lollini PL, Colombo MP, Forni G. Interleukin 12-mediated prevention of spontaneous mammary adenocarcinomas in two lines of Her-2/neu transgenic mice. J Exp Med 1998;188:589–596. [PubMed: 9687535]

23. Nahta R, Yu D, Hung MC, Hortobagyi GN, Esteva FJ. Mechanisms of disease: understanding resistance to HER2-targeted therapy in human breast cancer. Nat Clin Pract Oncol 2006;3:269–280. [PubMed: 16683005]

24. Chaussade C, Rewcastle GW, Kendall JD, Denny WA, Cho K, Gronning LM, Chong ML, Anagnostou SH, Jackson SP, Daniele N, Shepherd PR. Evidence for functional redundancy of class IA PI3K isoforms in insulin signalling. Biochem J 2007;404:449–458. [PubMed: 17362206]

25. Patrucco E, Notte A, Barberis L, Selvetella G, Maffei A, Brancaccio M, Marengo S, Russo G, Azzolino O, Rybalkin SD, Silengo L, Altruda F, Wetzker R, Wymann MP, Lembo G, Hirsch E. PI3Kgamma modulates the cardiac response to chronic pressure overload by distinct kinase-dependent and -independent effects. Cell 2004;118:375–387. [PubMed: 15294162]

26. Hirsch E, Lembo G, Montrucchio G, Rommel C, Costa C, Barberis L. Signaling through PI3Kgamma: a common platform for leukocyte, platelet and cardiovascular stress sensing. Thromb Haemost 2006;95:29–35. [PubMed: 16543958]

27. Jia S, Liu Z, Zhang S, Liu P, Zhang L, Lee SH, Zhang J, Signoretti S, Loda M, Roberts TM, Zhao JJ. Essential roles of PI(3)K-p110beta in cell growth, metabolism and tumorigenesis. Nature. 2008

28. Guillermet-Guibert J, Bjorklof K, Salpekar A, Gonella C, Ramadani F, Bilancio A, Meek S, Smith AJ, Okkenhaug K, Vanhaesebroeck B. The p110beta isoform of phosphoinositide 3-kinase signals

downstream of G protein-coupled receptors and is functionally redundant with p110gamma. Proc Natl Acad Sci U S A 2008;105:8292–8297. [PubMed: 18544649]

29. Biddinger SB, Kahn CR. From mice to men: insights into the insulin resistance syndromes. Annu Rev Physiol 2006;68:123–158. [PubMed: 16460269]
30. Ozanne SE, Jensen CB, Tingey KJ, Martin-Gronert MS, Grunnet L, Brons C, Storgaard H, Vaag AA. Decreased protein levels of key insulin signalling molecules in adipose tissue from young men with a low birthweight: potential link to increased risk of diabetes? Diabetologia 2006;49:2993–2999. [PubMed: 17063325]
31. Foukas LC, Beeton CA, Jensen J, Phillips WA, Shepherd PR. Regulation of phosphoinositide 3-kinase by its intrinsic serine kinase activity in vivo. Mol Cell Biol 2004;24:966–975. [PubMed: 14729945]
32. Hynes NE, Lane HA. ERBB receptors and cancer: the complexity of targeted inhibitors. Nat Rev Cancer 2005;5:341–354. [PubMed: 15864276]
33. Saal LH, Holm K, Maurer M, Memeo L, Su T, Wang X, Yu JS, Malmstrom PO, Mansukhani M, Enoksson J, Hibshoosh H, Borg A, Parsons R. PIK3CA mutations correlate with hormone receptors, node metastasis, and ERBB2, and are mutually exclusive with PTEN loss in human breast carcinoma. Cancer Res 2005;65:2554–2559. [PubMed: 15805248]
34. Carbone R, Fre S, Iannolo G, Belleudi F, Mancini P, Pelicci PG, Torrisi MR, Di Fiore PP. eps15 and eps15R are essential components of the endocytic pathway. Cancer Res 1997;57:5498–5504. [PubMed: 9407958]
35. Brachmann SM, Ueki K, Engelman JA, Kahn RC, Cantley LC. Phosphoinositide 3-kinase catalytic subunit deletion and regulatory subunit deletion have opposite effects on insulin sensitivity in mice. Mol Cell Biol 2005;25:1596–1607. [PubMed: 15713620]
36. Taniguchi CM, Kondo T, Sajan M, Luo J, Bronson R, Asano T, Farese R, Cantley LC, Kahn CR. Divergent regulation of hepatic glucose and lipid metabolism by phosphoinositide 3-kinase via Akt and PKClambda/zeta. Cell Metab 2006;3:343–353. [PubMed: 16679292]
37. Mora A, Lipina C, Tronche F, Sutherland C, Alessi DR. Deficiency of PDK1 in liver results in glucose intolerance, impairment of insulin-regulated gene expression and liver failure. Biochem J 2005;385:639–648. [PubMed: 15554902]
38. Quaglino E, Rolla S, Iezzi M, Spadaro M, Musiani P, De Giovanni C, Lollini PL, Lanzardo S, Forni G, Sanges R, Crispi S, De Luca P, Calogero R, Cavallo F. Concordant morphologic and gene expression data show that a vaccine halts HER-2/neu preneoplastic lesions. J Clin Invest 2004;113:709–717. [PubMed: 14991069]
39. We thank Valentina Spaziani, Laura Virgili and Laura Braccini for technical help; Peter Shepherd for inhibitors; Guido Tarone and Bart Vanhaesebroeck for constructive discussions. This work was supported by a grant from University of Torino (ex 60%), PRIN, Telethon, Italian Association for Cancer Research (AIRC) to E.H. and G.F., the Sixth Framework Programme EUGeneHeart and Fondation Leducq to E.H, NIH GM55692 to J.M.B., the EU FP6 grant BBW 03.0441-3/LSHG-CT-2003–502935 and Swiss Natl. Foundation grant 3100A0–109718 to M.P.W.
www.sciencesignaling.org/cgi/content/full/1/36/ra3/DC1

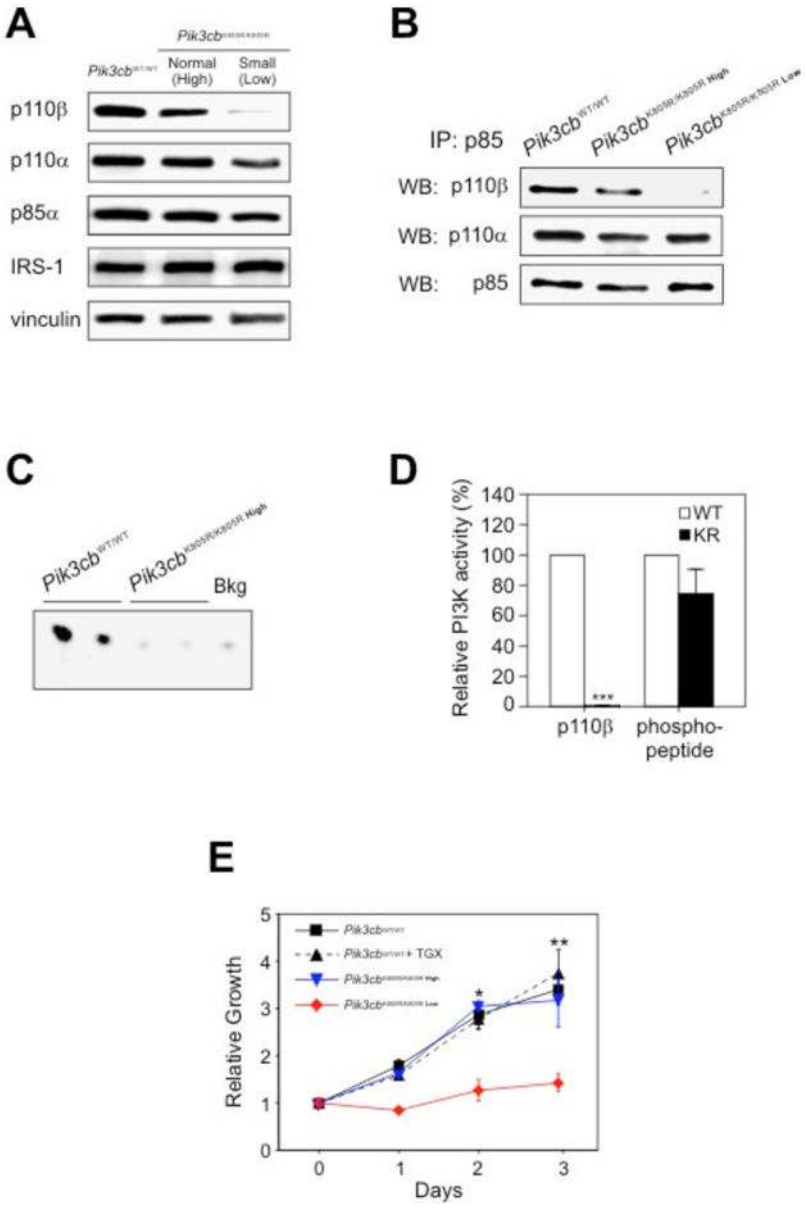

Fig. 1.

Kinase-dependent and independent functions of p110β in wild-type (*PIK3CB*$^{WT/WT}$) and *PIK3CB*$^{K805R/K805R}$ MEFs. A) *PIK3CB*^{K805R} gene dosage inversely correlates with phenotype severity. MEFs were derived from apparently normal (*PIK3CB*$^{K805R/K805R\ High}$) or abnormal (*PIK3CB*$^{K805R/K805R\ Low}$) 13.5 days post conception (d.p.c.) *PIK3CB*$^{K805R/K805R}$ embryos. Homogenates of MEFs of the described phenotypes were analyzed by SDS–PAGE and immunoblotted with the indicated antibodies. B) Analysis of p85 association to p110 in MEFs. Protein extracts were immunoprecipitated with anti-pan p85 antibodies and immunoblotted using the indicated antibodies. C) Analysis of p110β catalytic activity. Representative lipid kinase assay with p110β immunoprecipitated from wild-type or *PIK3CB*$^{K805R/K805R\ High}$ MEFs. D) PI3K activity in *PIK3CB*$^{K805R/K805R\ High}$ (KR) MEFs relative to that in wild type controls (WT), as measured after pull down with anti-p110β antibodies or with phosphopeptide-bound beads associating with all class IA PI3Ks. Asterisks: $P < 0.001$. E)

Proliferation curve of mutant MEFs with high and low p110β^{K805R} expression levels compared to that of wild-type MEFs with or without 100 nM TGX-221 treatment (TGX). Statistical significance: *PIK3CB*$^{K805R/K805R\ Low}$ cells vs. all other conditions (* $P < 0.05$, ** $P < 0.01$); other pairs of datasets: not significant.

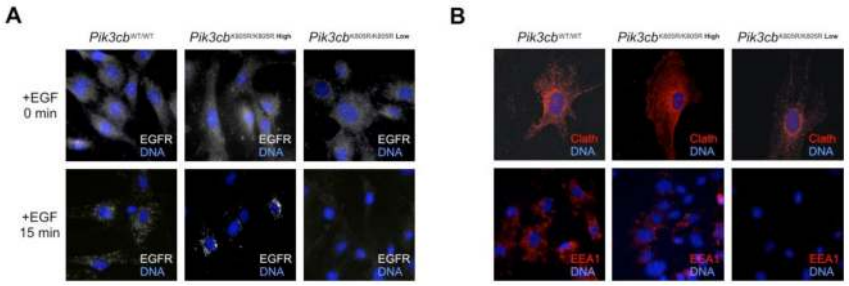

Fig. 2.

Analysis of EGF receptor endocytosis. A) Immunofluorescence of cells of the given genotype incubated with EGF for 1 hour at 4°C (0 min) and then shifted to 37°C for 15 minutes (15 min). Merged images show EGFR in white and 4′-6-Diamidino-2-phenylindole (DAPI) in blue. Exposure times were identical for the different genotypes but longer at 0 min to better show cell surface EGFR. B) Immunofluorescence of cells of the given genotype with anti-clathrin (top) or anti-EEA1 antibodies. Merged images show clathrin or EEA1 in red and DAPI in blue.

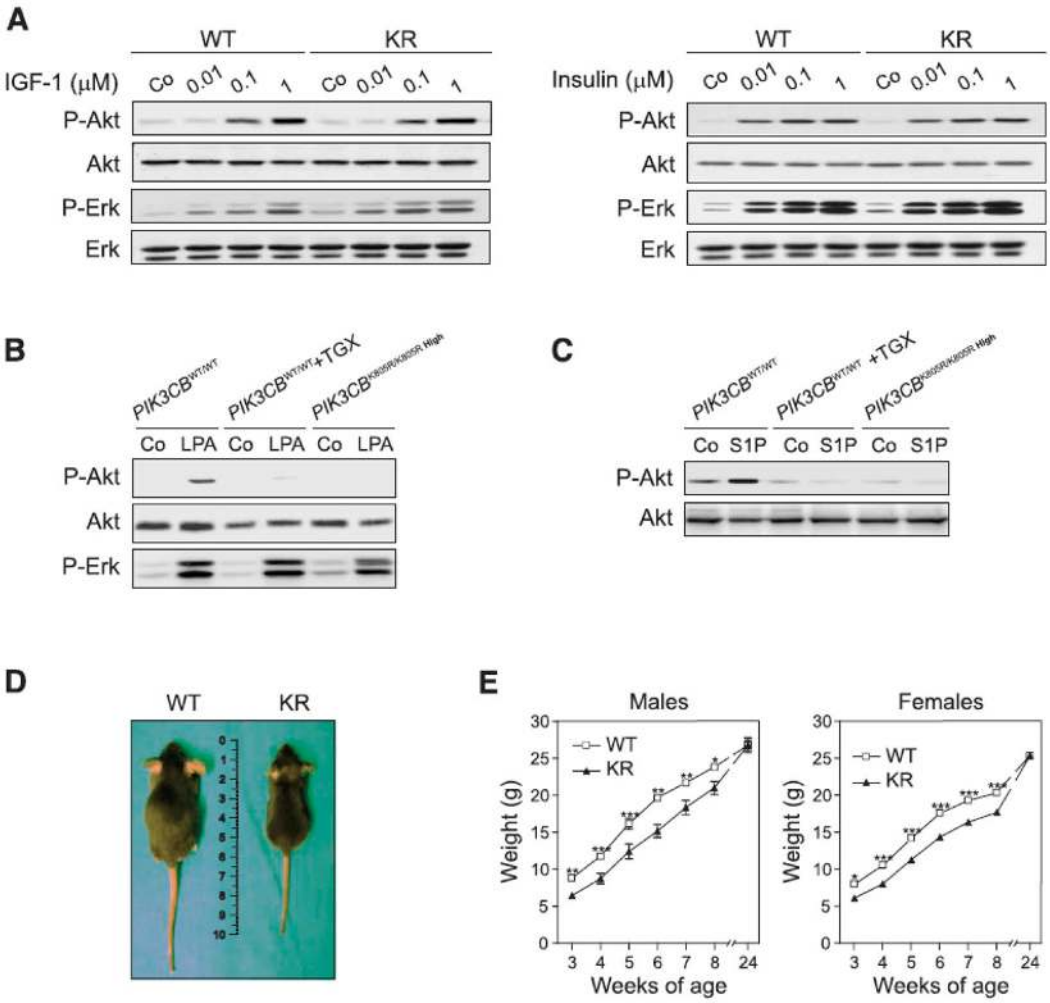

Fig. 3.

In vitro and in vivo consequences of p110β kinase-dead expression. A) IGF-1 and insulin-dependent Akt (also known as Protein kinase B, PKB) and extracellular signal regulated kinase 1 and 2 (Erk1/2) phosphorylation in wild-type (WT) and kinase-dead (KR) MEFs derived from normal embryos. Shown is a representative Western blot of eight independent experiments analyzing the response at 5 minutes after stimulation. B) Analysis of Akt phosphorylation after stimulation with LPA. Wild-type (WT) and *PIK3CB*$^{K805R/K805R\ High}$ MEFs were stimulated with 10μM LPA in the absence or presence of 100 nM TGX-221. C) Analysis of Akt phosphorylation 5 minutes after stimulation with S1P of cells of the indicated genotype in the presence or absence of the p110β inhibitor TGX221. Shown is a representative Western blot of three independent experiments. D) Growth analysis of *PIK3CB*$^{K805R/K805R}$ (KR) mice. The figure shows the external appearance of 6 week-old wild-type (WT) and *PIK3CB*$^{K805R/K805R}$ (KR) mice. E) Weight gain curve of wild-type (WT) and *PIK3CB*$^{K805R/K805R}$ (KR) mice from 3 to 24 weeks after birth (males n=13, females n=22; * $P < 0.05$, ** $P < 0.01$, ** $P < 0.001$).

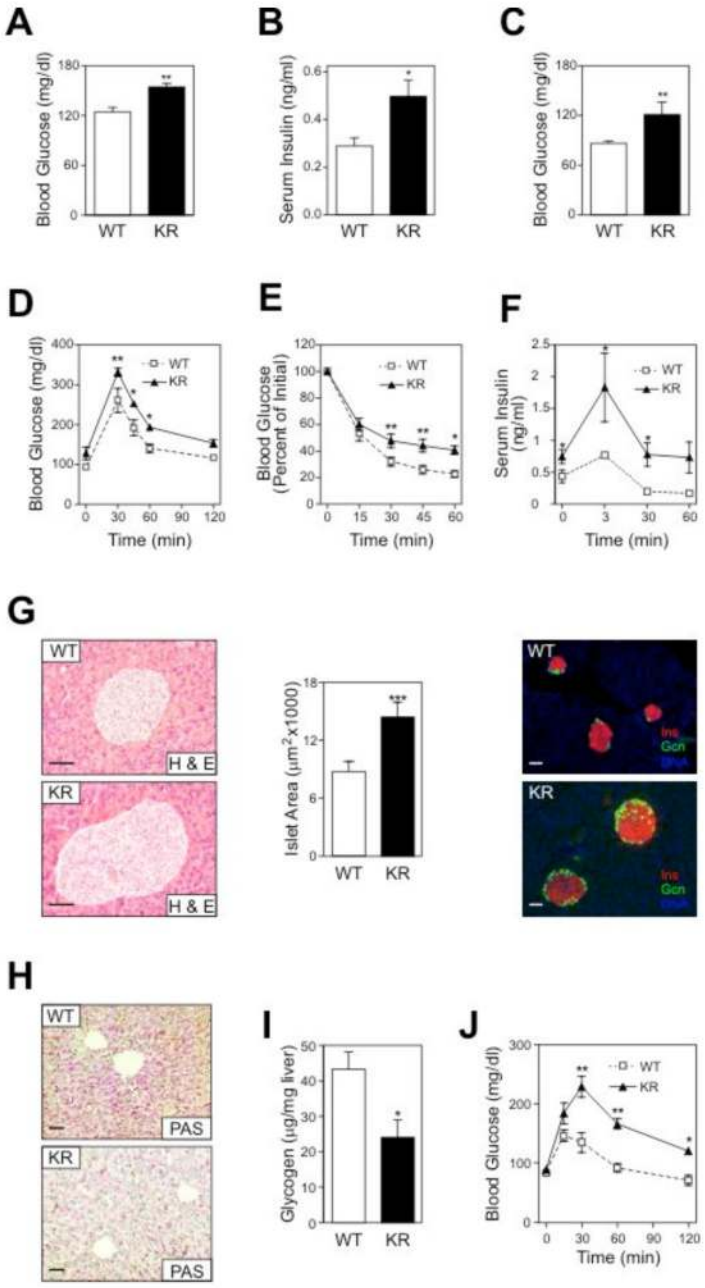

Fig. 4.

Insulin-dependent glucose metabolism in 6-month old wild-type (WT) and *PIK3CB*$^{K805R/K805R}$ mice (KR). Statistical significance: * $P < 0.05$, ** $P < 0.01$, ** $P < 0.001$. A) Blood glucose in random fed mice (n=9 per genotype). B) Insulin concentrations in the serum of random fed mice (n=9 per genotype). C) Blood glucose in fasted mice (wild type, n=9; KR, n=6). D) Glucose tolerance test (n=5 per genotype). E) Insulin tolerance test (n=7 per genotype). F) Insulin concentration in serum of glucose-treated fasted animals. G) Analysis of pancreatic islet size. Left: histological sections of hematoxylin-eosin (H & E) stained pancreata. Center: quantification of islet area (n=4 per genotype). Right: immunofluorescence with antibodies directed against insulin (Ins; red) and against glucagon (Gcn; green). Nuclei were stained with bisbenzimide (DNA; blue). Bars represent 100 μm. H) Histology of a

representative liver section of the indicated mice stained with the periodate-Schiff (PAS) stain, recognizing carbohydrates. Measurement of % of PAS positive pixels: WT: 7.3 ± 0.9; KR: 2.27 ± 0.4. I) Glycogen levels in the liver of randomly fed 24 week-old mice (n=7). J) Pyruvate challenge of wild-type (WT) and *PIK3CB*$^{K805R/K805R}$ (KR) mice. A bolus of 2 g/kg was administered intraperitoneally in 24 week-old mice fasted for 16 hours and blood glucose was measured at the indicated time points (n=5).

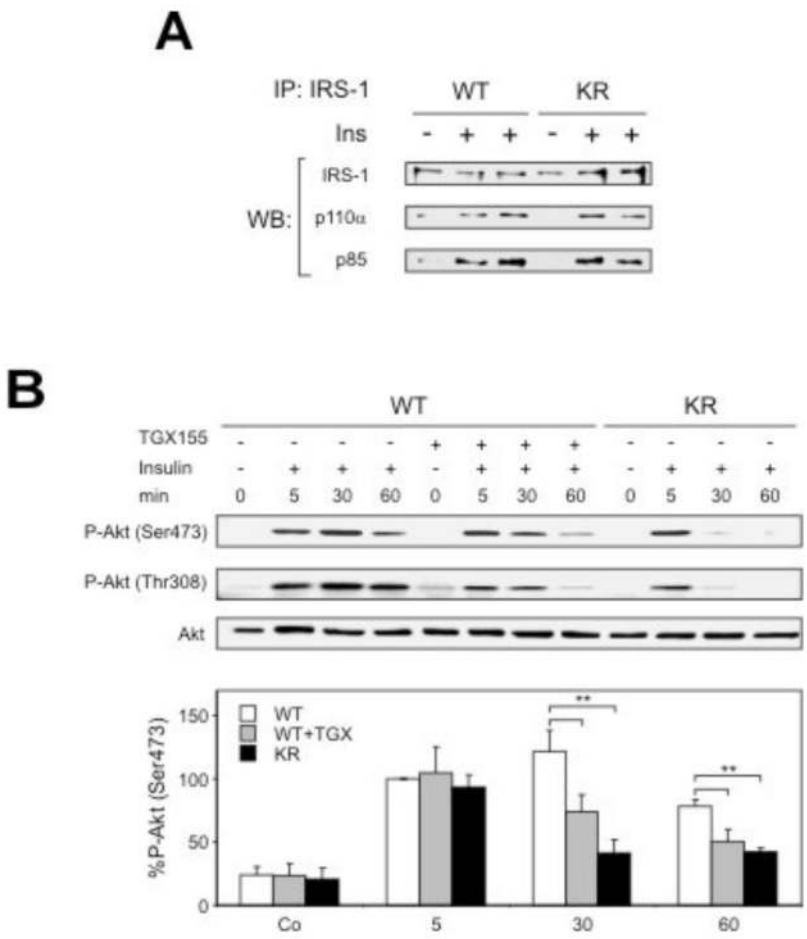

Fig. 5.

Role of p110β in insulin signaling. A) Insulin-induced recruitment to IRS-1 of p85 and p110α, determined by IRS-1 immunoprecipitation followed by immunoblot, 5 min after insulin stimulation of livers. B) Phosphorylation of Akt (on Thr308 and Ser473) determined by immunoblot, in livers of mice of the indicated genotype with and without TGX-155 treatment. Lower panel: quantification of Akt phosphorylation on Ser473 (n=5; ** $P < 0.01$).

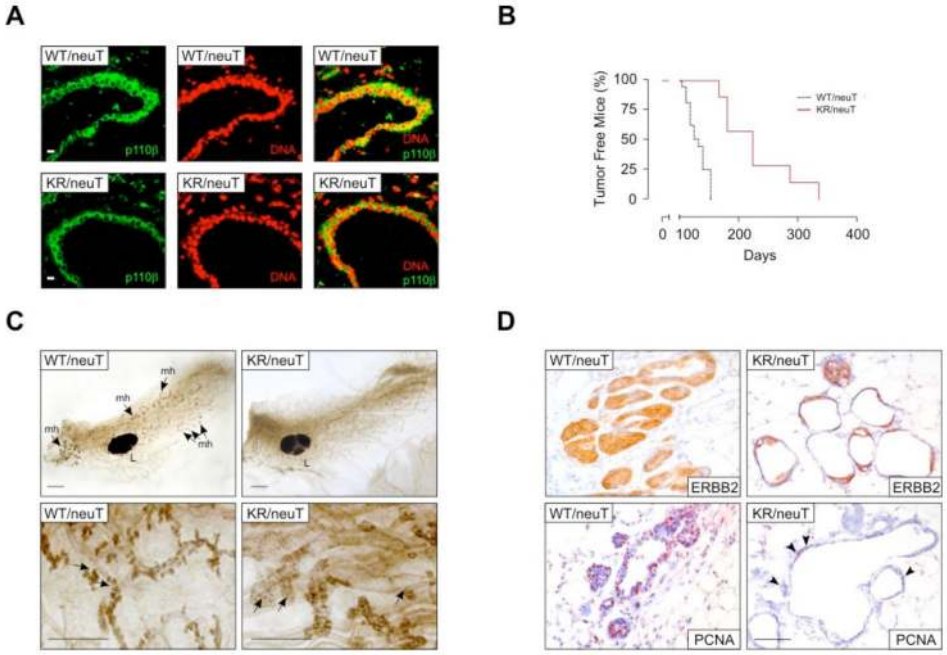

Fig. 6.

p110β is required for *ERBB2*-driven breast cancer development. A) p110β expression in mammary gland epithelium. Cryostat sections of mammary glands derived from *PIK3CB*$^{K805R/K805R}$/neuT (KR/neuT) and *PIK3CB*$^{+/+}$/neuT (WT) virgin females were stained with the anti-p110β 5g9 monoclonal antibody directly coupled to Alexa 488 (described in Suppl. Fig. 2d; green) as well as with the nuclear stain propidium iodide (red) and analyzed by confocal microscopy. Bar corresponds to 20 μm. B) Kinetics of tumor appearance in *PIK3CB*$^{WT/WT}$/neuT (WT/neuT; black lines; n=10) and *PIK3CB*$^{K805R/K805R}$/neuT (KR/neuT; red lines; n=7) compound mutant mice (*P*=0.01). C) Whole mount preparations of *PIK3CB*$^{WT/WT}$/neuT and *PIK3CB*$^{K805R/K805R}$/neuT mammary glands at 10 weeks. Upper panel: *PIK3CB*$^{K805R/K805R}$/neuT mammary gland shows a reduction of duct side buds constituted by atypical hyperplastic lesions. Lower panel: magnification of the side buds revealing the empty aspect of *PIK3CB*$^{K805R/K805R}$/neuT hyperplastic lesions. L: lymph node, mh: atypical mammary hyperplasia. Bar corresponds to 1 mm. D) Histology of mammary glands. Ducts were stained with anti Erbb2 and with anti PCNA antibodies to show transgene expression and proliferating cells, respectively. Bar represents 100 μm. Arrowheads indicate PCNA-positive cells in the mutant sample.

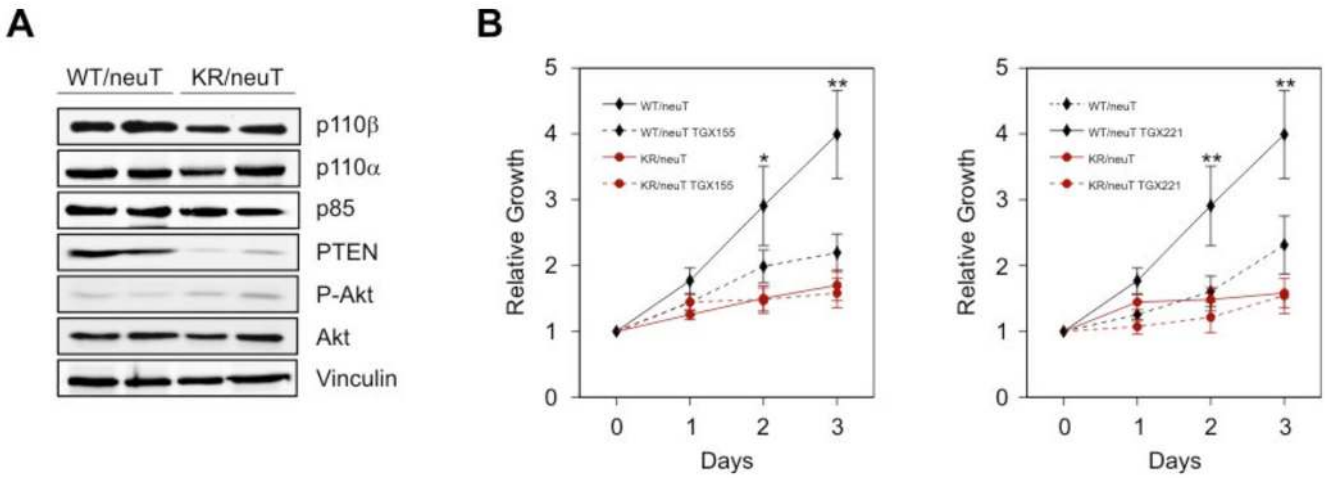

Fig. 7.

p110β kinase activity is required for *ERBB2*-driven breast cancer cell proliferation. A) Western blot analysis of protein expression in cultured mammary tumors of the two genotypes with the indicated antibodies. B) Proliferation curves, reported as relative increase in the number of cells compared to the initial seeding density, of cultured tumor cells of the two genotypes in the absence or presence of the p110β selective inhibitors TGX-155 (10 μM) and TGX-221 (100 nM). Statistical significance: wild-type cells vs. all other conditions (* $P < 0.05$, ** $P < 0.01$); other pairs of datasets: not significant.

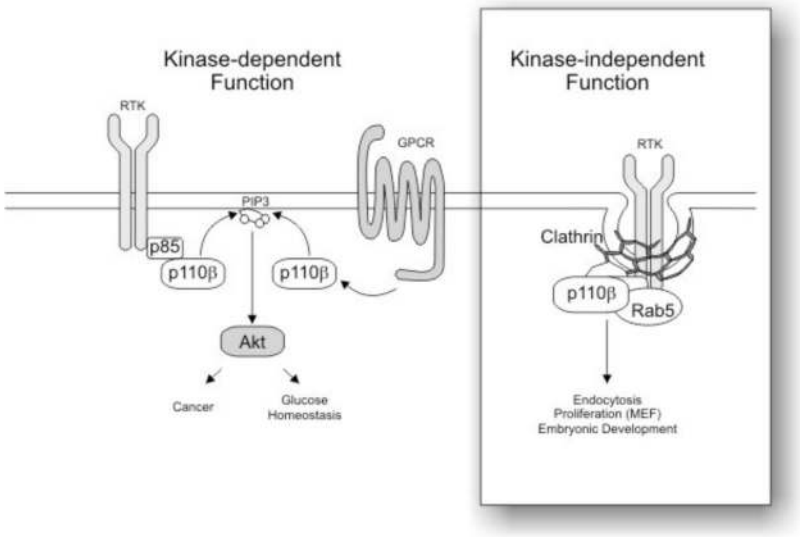

Fig. 8.

Model of the catalytic and non-catalytic functions of p110β. The catalytic activity of p110β is triggered by both RTK and GPCR signaling and cooperates in Akt activation, cancer development and glucose homeostasis (left side). p110β also functions as a scaffold protein (right inset) required for the organization at the plasma membrane of clathrin coated pits or vesicles, thus controlling RTK endocytosis.

Table I

Metabolic measurements in *Pik3cb*$^{K805R/K805R}$ Mice

	PIK3CB$^{WT/WT}$	*PIK3CB*$^{K805R/K805R}$	*P by Student t*
Triglycerides (mg/dL)	109±11	71±6	<0.05
Cholesterol (mg/dL)	66±3	45±2	<0.01
Free Fatty Acids (mM)	1.5±0.1	1.4±0.1	NS
AST (UI)	78±16	63±8	NS
ALT (UI)	47±12	37±3	NS
Plasma Albumin (g/dL)	2.3±0.1	2.2±0.1	NS
Leptin (ng/ml)	0.72±0.08	0.69±0.09	NS
Cumulative Food Intake (g food/q BW per 10 days)	0.30±0.02	0.27±0.01	NS
SREBF1C mRNA (% of WT)	100	72±4	<0.01
PCK1 mRNA (% of WT)	100	147±6	<0.01
G6PC mRNA (% of WT)	100	172±1	<0.01
FBP1 mRNA (% of WT)	100	134±7	<0.01

AST (aspartate aminotransferase); ALT (alanine transaminase); SREBF1C (sterol regulator element-binding protein-1c); PCK1 (phosphoenolpyruvate carboxykinase-1); G6PC (glucose-6-phosphatase, catalytic subunit); FBP1 (fructose 1,6-bisphosphatase).

Table II

Autochthonous Carcinogenesis in *Pik3cb*$^{K805R/K805R}$/neuT Mice

	latency[a]	**survival**[b]	**growth**[c]
***Pik3cb*$^{WT/WT}$/neuT (n=39)**	174±5	207±17	33±12
***Pik3cb*$^{K805R/K805R}$/neuT (n=35)**	227±9	279±14	52±5
	p<0.0001	p=0.0134	p<0.05

[a,b,c]Time in days:([a])from the birth and the growth of a 2mm diameter tumor;([b])from the birth and the growth of a 8mm diameter tumor;([c])time required for a 2mm diameter tumor to reach a 8mm diameter. Growth from 8 to 10mm diameter was not significantly different (n=5 per genotype; not shown).

Statistical analysis: paired t test